

# A post-processing technique for addressing ‘irregular frequencies’ and other issues in the results from BEM solvers

Thomas Kelly<sup>\*</sup>, Iñaki Zabala<sup>\*\*</sup>, Yerai Peña-Sanchez<sup>†</sup>, Markel Penalba<sup>††</sup>, John V. Ringwood<sup>§</sup>, João C. C. Henriques<sup>‡</sup>, Jesús M. Blanco<sup>¶</sup>

**Abstract**—Within the wave energy community, hydrodynamic coefficients obtained from boundary element methods (BEMs) are commonly used to predict the behaviour of wave energy converters (WECs) in response to incident waves. A number of commercially-available BEM solvers exist, with a number of open-source alternatives also available. While open-source solvers have an obvious cost advantage compared to their commercial counterparts, the results from such solvers are often susceptible to so-called ‘irregular frequencies’, which arise from ill-conditioning in boundary integral problems, and result in large under- or over-estimation of hydrodynamic parameters at certain excitation frequencies. Furthermore, while commercial solvers may employ techniques to suppress the effects of irregular frequencies, such solvers may, under certain circumstances, exhibit other problems in the hydrodynamic results produced. For example, the results obtained for the added mass at high frequencies, and the infinite frequency added mass for a water column, may be incorrect. The current work first focusses on an approach to remove the effects of irregular frequencies from the results obtained for the radiation damping of a particular WEC geometry. The use of radiation damping results to obtain values for the added mass, through the use of the Ogilvie relations, is then considered. The technique described herein has been implemented in BEMRosetta, an open-source tool which allows a user to view the results from various BEM solvers, as well as converting input files between solvers. The results presented in this paper have been obtained using the BEMRosetta implementation.

**Index Terms**—Boundary element methods, Irregular frequencies, Numerical modelling

## I. INTRODUCTION

**N**UMERICAL models of proposed WECs are an essential design tool for the development of the ocean energy industry, not least for the prediction of the likely energy generated by a WEC,

and for the design of suitable model-based controllers/estimators/etc for WECs. The behaviour of a WEC may be modelled in either the frequency or time domains, and in single or multiple degrees of freedom, using the equations of motion for the WEC. The equations of motion are parameterised using frequency-dependent hydrodynamic coefficients including radiation damping and added mass. The hydrodynamic coefficients for a given geometry may be obtained from BEM solvers. A number of commercial solvers exist, including WAMIT [1], AQWA [2], and WADAM [3]. However, such commercial tools are relatively expensive, and many early-stage developers, and academic researchers, may prefer to make use of open-source BEM solvers, notably Nemoh [4], and, more recently, HAMS [5] and Capytaine [6] which can also provide satisfactory results [7]. All BEM solvers, commercial and open-source, may suffer from so-called irregular frequencies arising from ill-conditioning in the boundary integral problem, which can result in significant localised over- and under-predictions of the hydrodynamic parameters, localised at specific frequencies. It is important to note that, while this phenomenon is commonly referred to as an *irregular frequency*, (and this term is used to refer to the phenomenon throughout the current work), such localised over- and under-predictions of the hydrodynamic parameters are in no way due to the frequency, and indeed the frequency values themselves are in no way irregular. Rather it is the values for the hydrodynamic parameters around these frequencies that behave in an irregular manner compared to the adjacent values. Such over- and under-predictions, if left unattended, will result in inaccuracies in the predictions of the behaviour of a device modelled in the frequency domain in and around the irregular frequencies. Furthermore, Cummins’ equation [8], often used to model WECs in the time domain, estimates radiation forces using a convolution between the velocity or acceleration of the WEC and the corresponding impulse response function (IRF) of the radiation forces. The IRF of the radiation force in the time domain is commonly determined using either the frequency-dependent radiation damping or added mass, obtained from BEM solvers, in accordance with the Ogilvie relations [9]. The process of obtaining the IRF requires integration of either the added mass or radiation damping over a range of frequencies from zero to infinity. In practice, such integrations are truncated at a suitably high frequency, but any errors in

<sup>\*</sup>T. Kelly (e-mail: kellyt@dkit.ie) is with the Centre for Renewable Energy at Dundalk IT, Ireland

<sup>\*\*</sup>I. Zabala (e-mail: inaki.zabala@sener.es) is at SENER Ingeniería y Sistemas, S.A., Av. Zugazarte 56, 48930 Getxo, Spain

<sup>†</sup>Y. Peña-Sanchez (e-mail: yerai.pena.2017@mumail.ie), is at the Centre for Ocean Energy Research (COER), Maynooth University, Co. Kildare, Ireland

<sup>††</sup>M. Penalba(e-mail: mpenalba@mondragon.edu) is at the Mondragon University, Loramendi Kalea, 4. 20500 Arrasate, Spain

<sup>§</sup>J. Ringwood (e-mail: john.ringwood@mu.ie), is at the Centre for Ocean Energy Research (COER), Maynooth University, Co. Kildare, Ireland

<sup>‡</sup>J.C.C. Henriques (e-mail: joaochenriques@tecnico.ulisboa.pt) is at IDMEC, Instituto Superior Técnico, Universidade de Lisboa, Av. Rovisco Pais, 1049-001 Lisboa, Portugal

<sup>¶</sup>J.M. Blanco (e-mail: jesumaria.blanco@ehu.eus) is at the University of the Basque Country (UPV/EHU), Plaza Ingeniero Torres Quevedo 1, 48130 Bilbao, Spain

the hydrodynamics due to the presence of irregular frequencies will impact negatively on the resultant IRF.

Commercial solvers typically include built-in routines to eliminate, or at least mitigate, the presence of irregular frequencies in the generated output. Such techniques, which take place when solving the boundary value problem (as opposed to during a post-processing stage), typically work by closing a geometry at the free surface using the ‘lid method’ [10]. But, while steps have been made to implement such routines in some open-source solvers, irregular frequencies remain a significant issue for some solvers, notably Nemoh, and solvers derived from Nemoh, such as Capytaine. Furthermore, commercial solvers may, under certain circumstances, exhibit other problems in the hydrodynamic results produced; for example, there are commonly issues with the results for the high-frequency added mass and infinite frequency added mass for an oscillating water column (OWC) obtained from the commercial solver WAMIT. In the methods outlined in this paper, no attempt is made to prevent the occurrence of irregular frequencies, or other related issues present in the hydrodynamic results in the output from BEM solvers. Rather, post-processing techniques to subsequently address irregular frequencies (and other issues) are described, and the results from applying these techniques to some typical test cases are illustrated.

The first part of the current work describes the issues that may arise with the hydrodynamics obtained from BEM solvers. The second part of this paper focusses on techniques to remove the effect of irregular frequencies from the results obtained from BEM solvers for the radiation damping of a geometry, while the third part focusses on the use of radiation damping results (either those directly obtained from the BEM solvers, or results which have been post-processed as above) to obtain values for the added mass through the use of the Ogilvie relations. The techniques described may also be used to improve the results obtained for the infinite frequency and high-frequency added mass values for OWCs obtained from some commercial solvers, or remove discontinuities in the added mass results which may sometimes arise in open-source solvers. As described in Section II, a number of different issues may arise with added mass results. While similar techniques as used to address issue with the radiation damping values could also be used to handle some issues with the added mass, the use of the Ogilvie relations to obtain the added mass from the radiation damping may be used to address all the issues with added mass results described in Section II.

## II. ISSUES WITH HYDRODYNAMICS FROM BEM SOLVERS

### A. Irregular frequencies in the radiation damping

Irregular frequencies in a radiation damping curve commonly manifest as large, localised increases (or decreases) in the values obtained for the damping as the frequency increases. These increases (or decreases) in the damping value deviate significantly from the

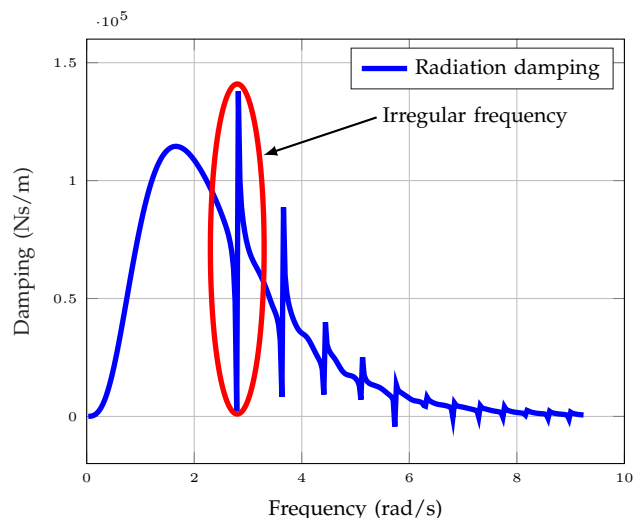


Fig. 1. An example of irregular frequencies in the radiation damping for an ellipsoid in heave, obtained from Nemoh, showing large, localised increases and decreases in the damping values.

values that might be expected when considering the surrounding damping values. This is followed immediately by similarly-sized sudden decreases (or increases) in the expected value. Finally, the overall trend of the radiation damping curve reverts to the trajectory it was following prior to the irregular frequency event. Figure 1 illustrates a typical set of radiation damping results obtained for an ellipsoid in heave from the open-source BEM solver Nemoh which contains irregular frequencies; one such irregular frequency is circled. Irregular frequencies in the radiation damping curve can also take the forms illustrated in Figures 2 and 3. Figure 2 illustrates the radiation damping for a hemispherical float in pitch where the irregular frequencies take the form of numerous relatively small and localised increases only as frequency increases before returning to the expected values. Figure 3 illustrates the radiation damping for a cube in roll where the irregular frequencies take the form of numerous relatively small and localised decreases only. The radiation damping values in Figures 2 and 3 were also obtained from Nemoh.

### B. Irregular frequencies in the added mass

Irregular frequencies may also manifest in results obtained from BEM solvers for the frequency-dependent added mass for a geometry. Figure 4 illustrates the added mass obtained from Nemoh for the same ellipsoid for which the radiation damping is illustrated in Figure 1. As in the radiation damping curve, similar, significant, localised variations in the values for the added mass can be seen corresponding to each irregular frequency event. Note that the irregular frequency issues occur at the same frequencies in both the added mass and radiation damping.

### C. Discontinuities in the added mass

Another issue which may arise in the frequency-dependent added mass curves is the presence of discontinuities in the data. This issue appears to primarily

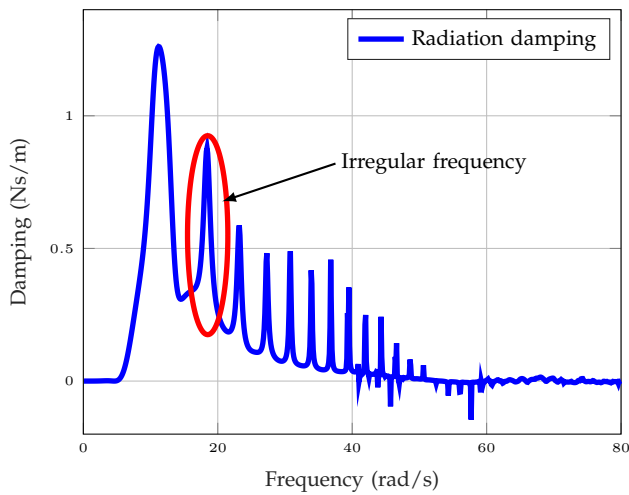


Fig. 2. An example of irregular frequencies in the radiation damping for a hemispherical float in pitch, obtained from Nemoh, showing localised increases in the damping values.

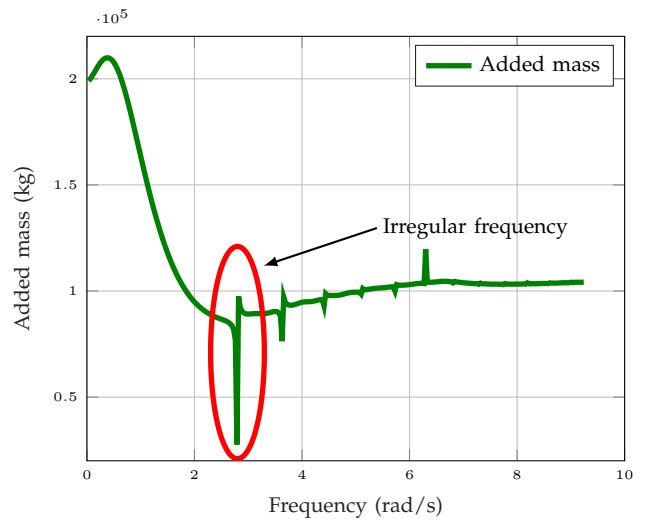


Fig. 4. An example of irregular frequencies in the added mass for an ellipsoid in heave, obtained from Nemoh, showing localised increases and decreases in the added mass values.

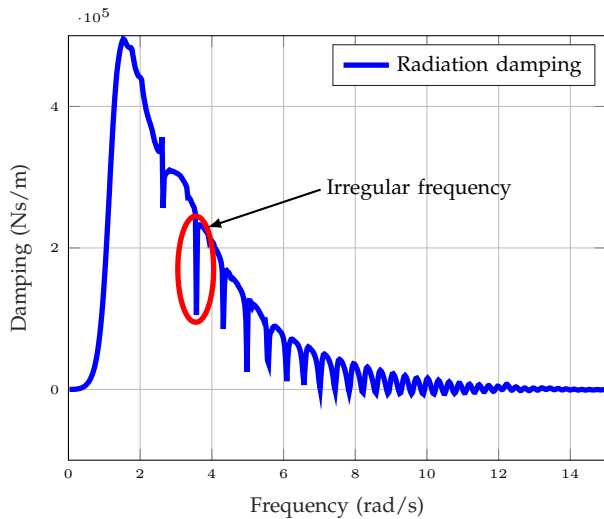


Fig. 3. An example of irregular frequencies in the radiation damping for a cube in roll, obtained from Nemoh, showing localised decreases in the damping values.

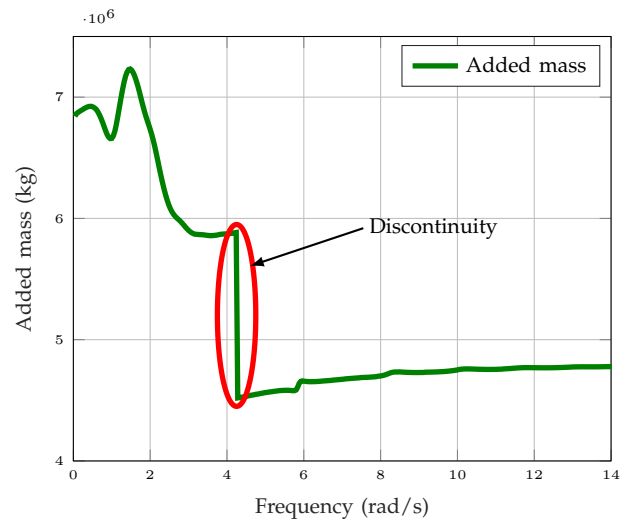


Fig. 5. Added mass for an OSWEC-type device, obtained from Capytaine, illustrating a discontinuity in the added mass curve for the pitch mode.

affect open-source solvers, and Figure 5 illustrates an example of this phenomenon for the added mass in the pitch mode of an oscillating surge wave energy converter-type (OSWEC) device obtained from Capytaine.

*D. High-frequency added mass issues for OWCs*

An issue which is specific to the hydrodynamics obtained by commercial BEM solvers when used to model OWCs arises when the so-called massless disc approach is employed. The piston mode of the water column is represented by the heave motion of an infinitely-thin, massless disc located on the water surface. Due to the thin nature of this disc, BEM solvers incorrectly calculate the added mass at high frequencies, which, instead of being asymptotic to the infinite frequency added mass, will tend to minus infinity. The modelling process can be extended to the sloshing modes of the OWC, and it is also common to find the added mass for sloshing modes tending to plus

infinity. Furthermore, BEM solvers often fail to estimate the appropriate value for the infinite frequency added mass in these cases. Figure 6 illustrates an example of this issue for the piston mode of an OWC using added mass values obtained from WAMIT. The tendency of the added mass curve at high frequencies to approach minus infinity can be clearly seen, as indeed can the presence of some irregular frequencies at higher frequencies.

While discontinuities in the added mass, and the issue with high-frequency added mass values for an OWC, are not caused by irregular frequencies, both are included here as the same technique used to remove irregular frequencies described herein may also be used to address these issues.

III. POST PROCESSING THE RADIATION DAMPING

Two methods for post processing the radiation damping obtained from BEM solvers have been implemented in the open-source tool, BEMRosetta. The first

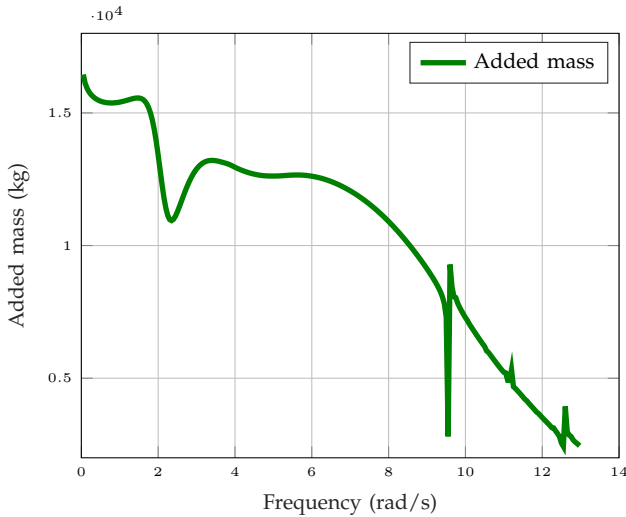


Fig. 6. Added mass for an OWC, obtained from WAMIT, illustrating the trend toward minus infinity at high frequencies, and some irregular frequencies.

method is to apply low-pass filtering to the radiation damping data. The second approach is, to the authors' knowledge, novel to the current implementation and is described in Section III-B.

#### A. Low-pass filtering

A forward and reverse, low-pass Butterworth filtering process may be applied to radiation damping results in BEMRosetta. During the forward pass, the data is filtered and the irregular frequencies removed based on a user-defined cut-off frequency. The forward pass will introduce a phase offset, which will cause the radiation damping curve to shift with respect to frequency. The filtered data is then reverse passed through the filter to remove the phase offset.

#### B. Novel approach to removing irregular frequencies

Low-pass filtering of the radiation damping data can successfully remove the effect of irregular frequencies from the radiation damping obtained from BEM solvers in many cases. However, a robust automatic selection process to determine suitable cut-off values for the filter, which removes the effects of irregular frequencies without leaving significant artifacts and also without attenuating parts of the damping curve it is intended to retain, has, to-date, proven elusive. The desire to automate the process of irregular frequency removal to as large an extent as possible led to the development of a novel approach to removing the effect of irregular frequencies in hydrodynamic results. This novel approach to handling issues with the radiation damping and added mass values (described in Section II) has been implemented in BEMRosetta. The technique first processes the radiation damping values, before using the results obtained from either that process or the filtering process outlined in Section III-A, to obtain added mass results. The novel technique for removing the effect of irregular frequencies from the radiation damping comprises four main steps.

The raw data is first cleaned to ensure it is suitable for the subsequent steps. Next, a so-called 'Area of Interest' is defined to facilitate the selection of specific damping values (occurring at irregular frequencies) to be removed. The third step identifies the irregular frequencies within the data in the 'Area of Interest' and removes the radiation damping values at irregular frequencies in this data. The final step is to repair the gaps in the data which arise once the damping values for the irregular frequencies are removed, and to add a 'tail' to the damping curve for frequencies which lie beyond the 'Area of Interest'. Each step in the process is now described. Note that in the processes described below a number of critical parameters have been selected by a process of trial and error, and based on the observations and experience of the authors.

1) *Cleaning the raw data:* Cleaning of the raw radiation damping data is performed to ensure the data is in a suitable form for the remaining steps in the process. Firstly, any instances where the result obtained by the solver is undefined, which typically appear as *NaN* in the raw data, are removed from the data set. Secondly, as a user may define any frequencies they wish to be analysed by a BEM solver, it cannot be assumed that each frequency is represented only once, that the frequencies are in ascending or descending order or that the spacing between frequency points is uniform. Therefore, the algorithm checks for, and removes, any duplicate frequencies. The data is then sorted in order of ascending frequency, and re-sampled to ensure even spacing between the frequencies. The re-sampling routine creates a histogram of all the intervals between the frequencies in the data set. If one interval value occurs 80% (or greater) of the time, then that value is used to re-sample all the data. Otherwise, the mean value of all the intervals is used. Re-sampling is performed linearly.

2) *Defining the 'Area of Interest':* The novel technique identifies a range of frequencies, and a range of damping values within the data set, which define the so-called 'Area of Interest'. The width of this area is defined by upper and lower frequency values, while the height is bounded by zero and an upper value for the radiation damping. The width and height of the 'Area of Interest' are determined so as to encompass the majority of the radiation damping information, and will therefore vary depending on the geometry being analysed. The range of frequencies over which the 'Area of Interest' spans is determined using a two-stage process. The first step of the process depends on the area bounded between the radiation damping curve and the frequency axis. The low frequency limit is set to the frequency where the area bounded by a vertical line at the frequency, the radiation damping curve and the frequency axis is equal to, or greater than the 1<sup>st</sup> percentile of the total area. The upper limit is set equal to the frequency corresponding to the 98<sup>th</sup> percentile. The percentile values have been chosen based on experience. However, it is possible that large peaks due to irregular frequencies at high frequencies may result in an inappropriately high upper limit for the frequency range, which will adversely effect the

second stage of identifying the 'Area of Interest', which is the selection of the appropriate damping range. To prevent this, the algorithm next divides the frequency range defining the extent of the 'Area of Interest' thus far into 20 frequency segments of equal length. The average value of damping for each segment is checked in turn, starting from the lowest frequency, to ensure it is at least 5% of the maximum damping value. If the average damping value in a segment is below 5% of the maximum value, the segment, and all segments at higher frequencies, are not included in the 'Area of Interest', and the upper limit of the frequency range for the 'Area of Interest' is reset to the upper frequency of the last valid segment. It is worth noting that an upper limit for the frequency range that could be considered is the value at which the damping values returns to zero. However, this would prove problematic for cases with a double-peak radiation damping.

The second step in determining the 'Area of Interest' is to establish the range of damping values to consider. These values are determined by first applying a 3rd-order, low-pass Butterworth filter to the radiation damping data where the cut-off frequency is 20% of the frequency range used to define the width of the 'Area of Interest'. The lower limit of the damping values is set equal to zero, while the upper limit it set equal to the maximum value of the filtered damping. Figure 7 below illustrates an example of the 'Area of Interest' obtained for one data set.

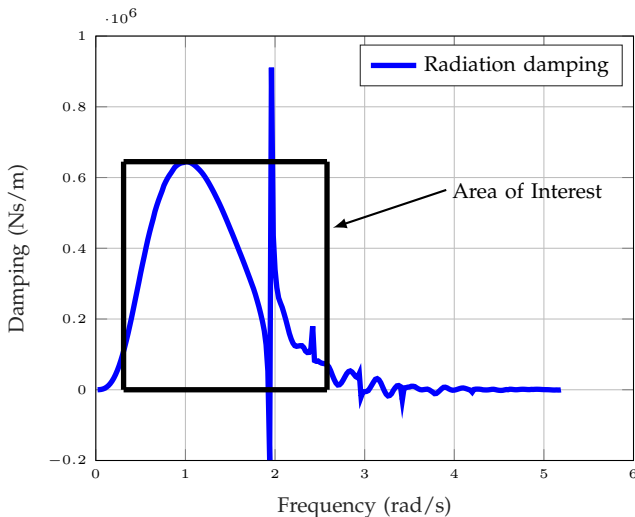


Fig. 7. Example of an 'Area of Interest' for a typical radiation damping data set.

3) *Identifying and removing peaks*: Two processes are used to identify peaks due to the effects of irregular frequencies within the damping data in order that the phenomena illustrated in Figure 1 and Figures 2 and 3 may be captured and resolved. The first process, used to remove the effects of irregular frequencies such as those illustrated in Figure 1, where large localised increases *and* decreases in the damping values occur, initially identifies all peaks and troughs within the 'Area of Interest'. Next, for each value of damping at a peak (or a trough), the value is compared to the adjacent values on both sides. If a difference of greater

than 20% of the upper damping limit defining the 'Area of Interest' is found between the peak (or trough) value and either of the adjacent values, the peak (or trough) is assumed to be a result of the effect of an irregular frequency. While a figure based only on experience, the value of 20% of the maximum 'Area of interest' has, to date, proven effective at identifying such peaks and troughs.

Once the peaks in the damping data due to the effects of irregular frequencies have been identified, the peak at the lowest frequency value is first removed. It is then necessary to determine how much damping data from either side of the irregular frequency should be removed. A frequency window of damping values to be removed is determined on the fractional height of the peak (or depth of the trough) to the height of the 'Area of Interest'. Specifically, the window width is set to 10% of the fractional height of the peak multiplied by the frequency width of the 'Area of Interest'. Again, the figure of 10% has been selected based on previous experience. Note that a maximum window to remove is set to 20% of the width of the 'Area of Interest' to prevent too much data being removed. Once the window around an irregular frequency has been removed, the height of the 'Area of Interest' is recalculated using the same process described in Section III-B2. Each peak identified as being due to the effect of an irregular frequency is removed in turn in order of the frequency of occurrence. As all data for frequencies beyond the 'Area of Interest' is replaced by an exponential tail, see Section III-B4, any peaks in the damping which lie beyond the 'Area of Interest' are, by default, removed.

If appropriate, a second process for identifying the effects of irregular frequencies addresses issues such as those illustrated in Figures 2 and 3 where localised increases (in the case of Figure 2), or localised decreases (in the case of Figure 3), in the damping values occur. Again, this process begins by identifying peaks and troughs, but only those which have a width of no more than 10% of the 'Area of Interest' and which occur at frequencies higher than that corresponding to the maximum damping value. When identified, the damping values which make up these irregular peaks are removed based on the local slope of the curve. A maximum allowable slope is calculated as six times the ratio of the height to the width of the 'Area of Interest'. If the local slope to the left of a peak exceeds the maximum allowable slope, these points are removed. Similarly, if the local slope to the right of a peak is more negative than minus the maximum allowed slope, these points are also removed. The reverse is true for troughs.

Finally, any negative damping values in the data set are discarded. Figure 8 illustrates an example of the results of this process as applied to the damping results shown in Figure 1 for an ellipsoid. Note the damping values associated with the the effects of irregular frequencies have been largely removed.

4) *Repairing the removed sections*: Once the damping values corresponding to the effects of irregular frequencies have been removed, the gaps in the damping data are interpolated. The nature of the interpolation

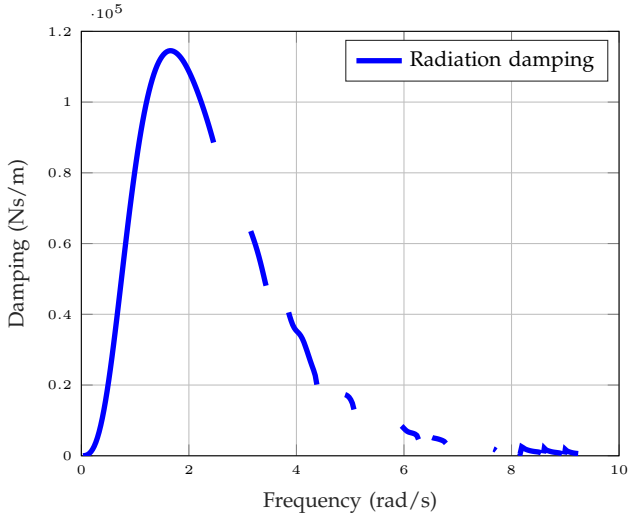


Fig. 8. Radiation damping curve corresponding to that in Figure 1 for an ellipsoid with the damping values associated with irregular frequencies removed as described.

performed depends on how large a specific gap in the damping data is. If the width of the gap is less than 10% of the width of the 'Area of Interest', a simple linear interpolation between the end points of the gap is performed. For larger gaps, a cubic curve is used to join the end points of the gap. The cubic curve joining larger gaps is constructed so that the slope of the start point (at the lower frequency) is the average value of the slope at the four previous points, while the slope at the end point where the curve rejoins the existing damping data is zero. It is intended that, in future updates to BEMRosetta, the slope at the start point will be the average of a number of points based on a percentage of the horizontal width of the 'Area of Interest', and also that the slope at the end point where the curve rejoins the existing damping will be determined by the average of the same number of points after the end point. Regardless of whether a removed section of the damping curve is replaced with a cubic or linear section, the algorithm attempts to smooth the transition between the existing data and the replacement sections. The smoothing process preserves the position and slope of the first point of the replacement section of the damping curve. A cubic spline is fitted from the third point *before* the first point of the replacement section, passes *through* the first point (the position of which is maintained) and ends at the third point *after* the first point. The coefficients of the cubic spline are obtained from the three points before and after the central point. A similar process is used to smooth the transition between the end point of the replacement section and the existing damping data.

Finally, the high-frequency tail of the damping curve, which lies outside the 'Area of Interest', is approximated by a decaying exponential. The tail extends from the final damping value within the 'Area of Interest' to a distance from the origin of one and a half times the width of the 'Area of Interest'. The join between the exponential tail and the remainder of the radiation damping curve is smoothed using the same technique

as is used to smooth the joints between interpolated data and the original, as described above. Figure 9 illustrates the results of the process as applied to the data in Figure 8. Note that the tail of the radiation damping curve has been replaced by the decaying exponential.

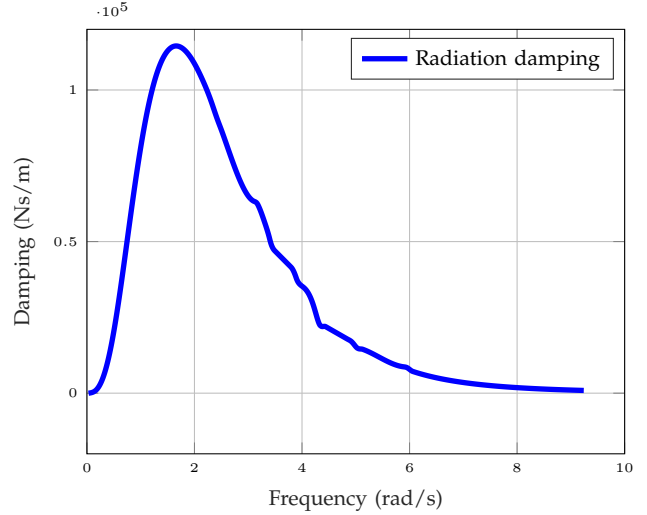


Fig. 9. Radiation damping curve for an ellipsoid with the effects of irregular frequencies removed, the gaps in the curve interpolated and smoothed, and a fitted exponential-based tail.

#### IV. POST PROCESSING THE ADDED MASS

A number of possible issues with the frequency-dependent added mass are illustrated in Section II. A single technique is implemented to address all the issues with the added mass which have been identified, i.e., the effects of irregular frequencies, discontinuities and the high-frequency issues in the added mass for OWCs. The technique is similar to that described in [11], but differs in how the infinite frequency added mass is determined. The process described herein of addressing issues with the added mass assumes that the frequency-dependent radiation damping values are free of the effects of irregular frequencies; if necessary the damping values may first be post processed as described in Section III. The radiation damping and added mass of a geometry are related to each other (and the impulse response of the radiation forces) through the well-known Ogilvie relations given in (1) and (2):

$$A(\omega) = A_{\infty} - \frac{1}{\omega} \int_0^{\infty} k(t) \sin(\omega t) dt \quad (1)$$

$$B(\omega) = \int_0^{\infty} k(t) \cos(\omega t) dt \quad (2)$$

where  $A_{\infty}$  is the so-called infinite frequency added mass, and  $k(t)$  is the radiation impulse response in the time domain, also known as the radiation kernel, and which contains the memory effect of the fluid response. Equation (2) allows  $k(t)$  to be expressed in terms of the frequency-dependent radiation damping as:

$$k(t) = \frac{2}{\pi} \int_0^{\infty} B(\omega) \cos(\omega t) d\omega \quad (3)$$

The technique to resolve issues with the added mass implemented in BEMRosetta first constructs the impulse response of the radiation forces from Equation (3), where the integration is calculated using Simpson's rule and is truncated at a sufficiently high frequency that the radiation damping curve has returned to zero, at which point the damping curve from higher frequencies will make no further contribution (assuming the range of frequencies available is sufficient that the damping curve has returned to zero). The added mass is then constructed from Equation (1). However, this operation requires knowledge of  $A_\infty$ . While some (but not all) BEM solvers will calculate a value for  $A_\infty$ , the technique employed herein does not assume knowledge of  $A_\infty$ . Instead, the added mass is first found from Equation (1) assuming  $A_\infty = 0$ . Next, the frequency corresponding to the maximum value of radiation damping is identified. For each value of the added mass, up to the frequency at which the maximum damping occurs, the value of  $A_\infty$  required to make the added mass obtained from (1), and the value obtained directly from the BEM solver equal to each other, is calculated. The final, single, value of  $A_\infty$  produced by the technique, and used to produce the added mass curve for all frequencies, is the average of all the values obtained for each value of the added mass up to the chosen frequency. The choice of the range of frequencies to consider when determining  $A_\infty$  is based on two observations in an attempt to ensure the robustness of the process. The first is that the effects of irregular frequencies typically manifest at frequencies higher than the frequency at which the maximum radiation damping occurs. The second observation is that the added mass curve for an OWC does not begin to exhibit the behaviour illustrated in Section II at frequencies lower than that at which the maximum damping occurs. The selection in this manner of the maximum frequency when determining the values to be averaged to obtain  $A_\infty$  ensures the values are not adversely biased by either phenomenon.

## V. SAMPLE RESULTS

Some examples of the results obtained using the techniques described herein to address the issues with the results from BEM solvers (illustrated in Section II) are now presented. Figure 10 overlays the radiation damping for an ellipsoid following the removal of the effects of irregular frequency on top of the unprocessed damping results obtained from Nemoh (previously illustrated in Figure 1). Figure 11 overlays the added mass for the ellipsoid following the removal of the effects of irregular frequency on top of the unprocessed added mass results (previously illustrated in Figure 4).

Figure 12 illustrates the result of applying the novel technique to process the radiation damping results for the OSWEC-type geometry (which was analysed with Capytaine to obtain the results previously illustrated in Figure 5), and using the processed damping values to obtain the added mass for the device. Note that the discontinuity in the added mass curve, clearly visible in the unprocessed results, has been addressed.

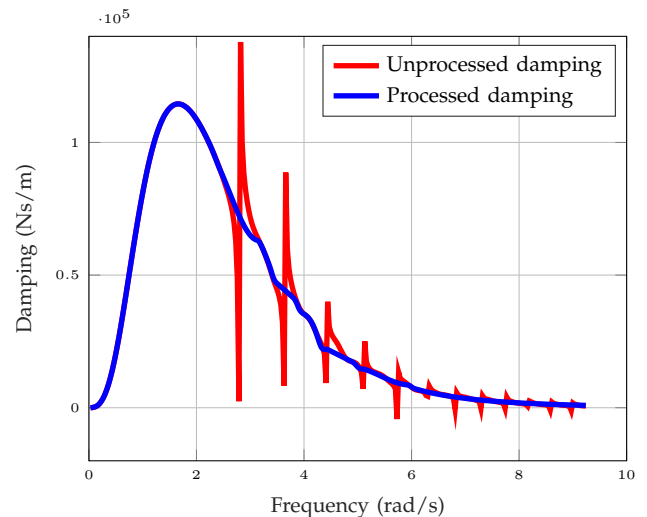


Fig. 10. Radiation damping curves for an ellipsoid before and after the effects of irregular frequencies have been processed by the techniques described herein.

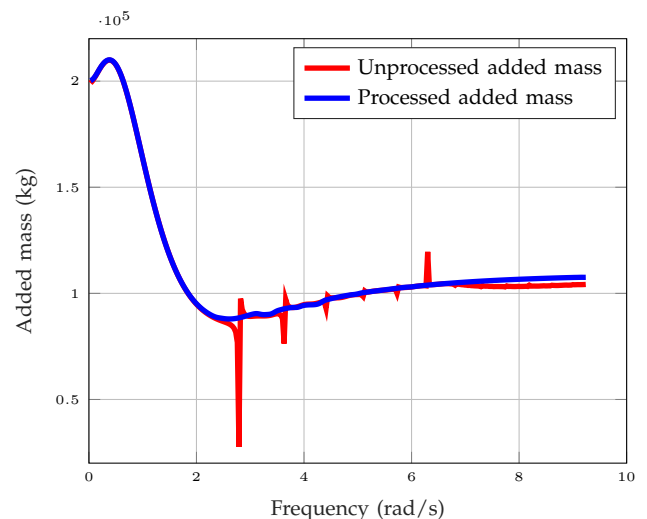


Fig. 11. Added mass curves for an ellipsoid before and after the effects of irregular frequencies have been processed by the techniques described herein.

Figure 13 illustrates the radiation damping results obtained for a bottom-mounted OWC from WAMIT. Note that the original results contain two large peaks at approximately 2 rad/s and 4 rad/s, as well as a low peak at approximately 7 rad/s. (The effects of some irregular frequencies can also be seen at high frequencies, but these occur after the damping has returned to zero and are at frequencies that would typically be beyond those of interest to a designer.) While processing the damping results as described herein has removed the effects of irregular frequencies at high frequencies, the algorithm has also removed entirely the third peak at 7 rad/s, which lies outside the 'Area of Interest' and which is not due to the effect of an irregular frequency. In this case it may in fact be better to use the original damping curve truncated at a suitably high frequency (e.g., by discarding values after 9 rad/s). Regardless, using either of the damping curves illustrated in Figure 13 to obtain the added mass curve produces virtually indistinguishable results for

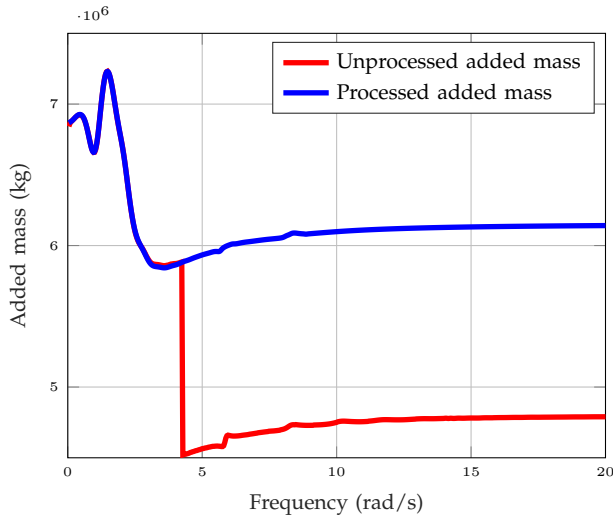


Fig. 12. Added mass curves for an OSWEC-type device in pitch before and after the added mass discontinuity was addressed.

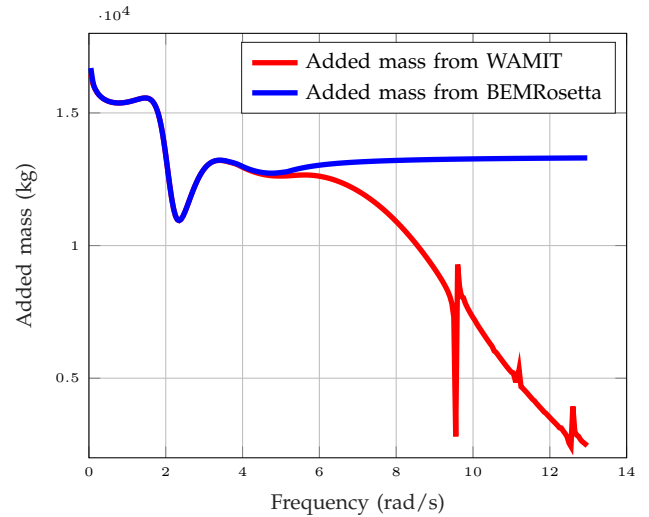


Fig. 14. Added mass curves for a bottom-mounted OWC obtained directly from WAMIT and as found using the techniques described herein.

the added mass.

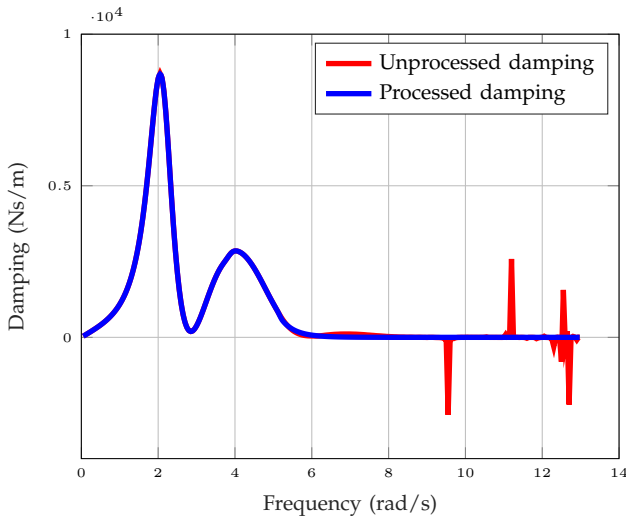


Fig. 13. Radiation damping curves for a bottom-mounted OWC, obtained from WAMIT, before and after the effects of irregular frequencies have been removed.

Figure 14 illustrates the comparison between the added mass results obtained directly from WAMIT for the same bottom-mounted OWC, and the added mass obtained from BEMRosetta using the radiation damping in conjunction with the Ogilvie relations and determining  $A_\infty$  as described in Section IV. Note the absence of the effects of any irregular frequencies in the processed results and also that the added mass no longer tends to minus infinity at high frequencies, but rather is asymptotic to the infinite frequency value. In this case, the value for  $A_\infty$  obtained from BEMRosetta is approximately 13,305 kg and the added mass curve illustrated in Figure 14 is asymptotic to this value.

The final set of results presented here in Figures 15 and 16 illustrates the radiation damping of a cuboid geometry, obtained from Nemoh, before the removal of the effects of irregular frequencies (which were previously illustrated in Figure 3) and the corresponding damping results after the effects of irregular frequen-

cies were removed. This is a particularly challenging set of results to process due to the large number of irregular frequency effects closely spaced together, and while the resultant radiation damping curve is an improvement on the original, it does retain artifacts of the effects of irregular frequencies following the removal process. The processed radiation damping results do, however, produce a clean impulse response function, which is then used to generate the added mass results presented in Figure 16.

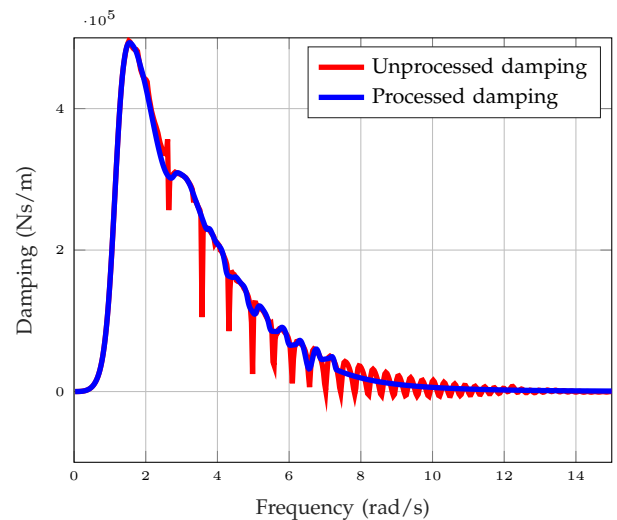


Fig. 15. Radiation damping curves for a cube before and after the effects of irregular frequencies have been removed.

## VI. FUTURE IMPROVEMENTS

The techniques described herein to mitigate the effects of irregular frequencies on the radiation damping and added mass results from BEM solvers have been implemented in BEMRosetta. However, the effects of irregular frequencies may also impact on the results obtained from BEM solvers for the wave-induced exciting forces. It is the intention of the authors that future releases of BEMRosetta may also include tools

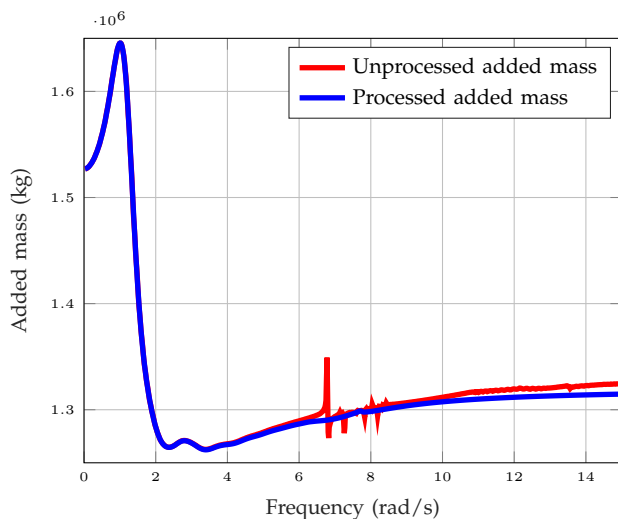


Fig. 16. Added mass curves for a cube before and after the effects of irregular frequencies have been removed.

to mitigate the effects of irregular frequencies on the exciting forces. One technique which is currently being investigated is the potential use of the 3-D Haskind relations [12] to obtain the exciting force from the radiation damping after the effects of the irregular frequencies on the radiation damping have been reduced for symmetrical bodies.

## VII. CONCLUSION

It is the hope of the authors that the post-processing techniques described herein, and implemented in the open-source tool BEMRosetta, may prove to be of use to the wider wave-energy community. The techniques have been extensively tested on multiple data sets generated from both commercial and non-commercial BEM solvers, for a wide range of geometries, in all rigid body modes of motion. To date, the techniques have proven robust and reasonably successful in removing the effects of irregular frequencies from the hydrodynamics obtained from BEM solvers, and in addressing the high-frequency added mass issues for OWCs. Although not shown here, the techniques have also been

tested on the results obtained for the coupled hydrodynamics between different modes for rigid bodies, and between multi-body systems. However, a number of critical parameters required by the algorithms are not determined *a priori*, but are based on the experience of the authors. Should users identify data sets where the techniques fail to improve the results directly obtained from BEM solvers, totally fail to remove the effects of irregular frequencies, or should any issues arise with the use of these tools, the authors would welcome correspondence on the matter.

## REFERENCES

- [1] "WAMIT," [www.wamit.com](http://www.wamit.com), 2021, [Online; accessed 02-January-2020].
- [2] "Ansys Aqwa," <https://www.ansys.com/products/structures/ansys-aqwa>, 2021, [Online; accessed 02-January-2020].
- [3] "Wave Analysis by Diffraction and Morison theory," <https://www.dnvgl.com/services/frequency-domain-hydrodynamic-analysis-of-stationary-vessels-wadam-2412>, 2021, [Online; accessed 02-January-2020].
- [4] A. Babarit and G. Delhommeau, "Theoretical and numerical aspects of the open source BEM solver Nemoh," in *11th European Wave and Tidal Energy Conference (EWTEC2015)*, Nantes, July 2015.
- [5] Y. Liu, "Hams: A frequency-domain preprocessor for wave-structure interactions—theory, development, and application," *Journal of Marine Science and Engineering*, vol. 7, no. 3, 2019.
- [6] M. Ancellin and F. Dias, "Capytaine: a python-based linear potential flow solver," *Journal of Open Source Software*, vol. 4, no. 36, p. 1341, 2019.
- [7] M. Penalba, T. Kelly, and J. Ringwood, "Using nemoh for modelling wave energy converters: A comparative study with wamit," in *12th European Wave and Tidal Energy Conference (EWTEC)*, 2017. [Online]. Available: <http://mural.maynoothuniversity.ie/12466/>
- [8] W. E. Cummins, "The impulse response function and ship motions," Navy Department, David Taylor Model Basin, DTNSRDC, Tech. Rep. 1661, October 1962.
- [9] T. Ogilvie, "Recent progress towards the understanding and prediction of ship motions." in *6th Symposium on Naval Hydrodynamics*, 1964.
- [10] Y. Liu and J. Falzarano, "Irregular frequency removal methods: Theory and applications in hydrodynamics," *Marine Systems & Ocean Technology*, vol. 12, 04 2017.
- [11] T. Kelly, T. Dooley, J. Campbell, and J. Ringwood, "Efforts towards a validated time-domain model of an oscillating water column with control components," in *Proceedings of the 11th European Wave and Tidal Energy Conference*, Nantes, France, 2015.
- [12] M. Haskind, "The exciting forces and wetting of ships in waves," *Izvestia Akademii Nauk S.S.S.R., Otdelenie Tekhnicheskikh Nauk*, No. 7, English translation, 1962 by J.N. Newman available as *David Taylor Model Basin Translation No. 307*, 1957.